Wind farm production estimates

Larsen, Torben J.; Larsen, Gunner Chr.; Aagaard Madsen , Helge; Hansen, Kurt Schaldemose

Published in:
Proceedings of EWEA 2012 - European Wind Energy Conference & Exhibition

Publication date:
2012

Document Version
Publisher's PDF, also known as Version of record

WIND FARM PRODUCTION ESTIMATES.

Torben J. Larsen
DTU Wind Energy
DK-4000 Roskilde
Denmark
Email: tjul@dtu.dk

Gunner Larsen
DTU Wind Energy
DK-4000 Roskilde
Denmark
Email: gula@dtu.dk

Helge Aagaard Madsen
DTU Wind Energy
DK-4000 Roskilde
Denmark
Email: hama@dtu.dk

Kurt S. Hansen
DTU Wind Energy
DK-2800 Kgs. Lyngby
Denmark
Email: kuhan@dtu.dk

ABSTRACT

In this paper, the Dynamic Wake Meandering (DWM) model is applied for simulation of wind farm production. In addition to the numerical simulations, measured data have been analyzed in order to provide the basis for a full-scale verification of the model performance.

The basic idea behind the DWM model is to model the instationary wind farm flow characteristics by considering wind turbine wakes as passive tracers continuously emitted from the wind farm turbines each with a downstream transport process dictated by large scale turbulent eddies (lateral and vertical transportation; i.e. meandering) and Taylor advection.

For the present purpose, the DWM model has been implemented in the aeroelastic code HAWC2 [1], and the performance of the resulting model complex is mainly verified by comparing simulated and measured loads for the Dutch off-shore Egmond aan Zee wind farm [2]. This farm consists of 36 Vestas V90 turbine located outside the coast of the Netherlands. The simulations in this paper were done with a modified version of HAWC2 only including aerodynamics and a rigid rotor in order to reduce the simulation time. With this code a 10min simulation takes approximately 1 minute on a 3GHz pc. The turbine controller is fully implemented. Initially, production estimates of a single turbine under free and wake conditions, respectively, are compared for (undisturbed) mean wind speeds ranging from 3m/s to 25m/s. The undisturbed situation refers to a wind direction bin defined as $270^\circ \pm 5^\circ$, whereas the wake situation refers to the wind direction bin $319^\circ \pm 5^\circ$. In the latter case, the investigated turbine operated in the wake of 6 upstream turbines, with the mean wind direction being equal to the orientation of the wind turbine row.

The production of the entire wind farm has been investigated for a full polar (i.e. as function of mean inflow wind direction). This investigation relates to a mean wind speed bin defined as $8m/s \pm 1m/s$. The impact of ambient turbulence intensity and turbine inter spacing on the production of a wind turbine operating under full wake conditions is investigated. Four different turbine inter spacings, ranging between 3.8 and 10.4 rotor diameters, are analyzed for ambient turbulence intensities varying between 2% and 20%. This analysis is based on full scale production data from three other wind farms Wieringermeer [3], Horns Rev [4] and Nysted [5]. A very satisfactory agreement between experimental data and predictions is observed.

This paper finally includes additionally an analysis of the production impact caused by atmospheric stability effects. For this study, atmospheric stability conditions are defined in terms of the Monin-Obukhov length. Three different stability classes, including stable, neutral and unstable atmospheric stratification, have been investigated.

1 INTRODUCTION

Production estimates of wind farms is a topic of utmost importance for obvious reasons. Due to computational limitations, wind farm production estimates have up to now entirely been based on a stationary description of the wind farm flow field, and a large number of models within this model segment have been proposed ranging from simple engineering models to fairly complex CDF based models.

The CFD models have typically taken the RANS approach based on some variant of the Boussinesq approximation. However, recently it was demonstrated [6] that the type of flow resulting from introduction of rotors in the atmospheric boundary layer (ABL) flows violates the assumptions of the Boussinesq approximation. This is basically because the turbulence length scale remains very large, whereas the changes of the flow are occurring over relatively smaller scales. The net effect is that the Reynolds stresses are largely overestimated both upstream and downstream the wind turbine, leading in turn to unrealistically high wake dissipation, which obviously is unfortunate.

One way to circumvent this fundamental problem is to adopt the approach of CFD Large Eddy Simulation (LES) for wind power estimation. This is, however, unfortunately horrendous computational expensive when all mean wind speeds and mean wind directions has to be included/considered. With the development of the "poor man's LES" often denoted as the dynamic wake meandering model (DWM) [7], a computational affordable approach is offered, which includes the basic features of the CFD LES approach in an engineering manner.

2 The DWM method

The Dynamic Wake Meandering (DWM) model complex is based on the combination of three corner stones; 1) modeling of quasi-steady wake deficits [8]; 2) a stochastic model of the down wind wake meandering; and 3) added - or self generated wake turbulence. The wake meandering part is based on a fundamental presumption stating that the transport of wakes in the atmospheric boundary layer can be modeled by considering the wakes to act as passive tracers driven by the large-scale turbulence structures in lateral and vertical directions [7]. Modeling of the meandering process consequently includes considerations of a suitable description of the "carrier" stochastic transport media as well as of a suitable definition of the cut-off frequency defining large-scale turbulence structures in this context. For the stochastic modeling of wake meandering, we imagine the wake as constituted by a cascade of wake deficits, each "emitted" at consecutive time instants in agreement with the passive tracer analogy [7], [9]. We then subsequently describe the propagation of each of the "emitted" wake deficits, and the collective description of these thus constitutes the wake meandering model. Adopting Taylor's hypothesis [10], the down-stream advection of these "emmisions" is assumed to be controlled by the mean wind speed of the ambient wind field. With this formulation the wake momentum in the direction of the mean flow is invariant with respect to down stream displacement. This is a considerable simplification allowing for a straight forward decoupling of the wake along wind deficit profile (and its expansion) and the wake transportation process. As for the dynamics in the lateral- and vertical directions, each considered wake cascade-element is displaced according to the large-scale lateral- and vertical turbulence velocities at the position of the particular wake cascade element at each time instant. The choice of a suitable stochastic turbulence field, that in turn defines the stochastic wake transport process, is not mandatory, but may be guided by the characteristics of the atmospheric turbulence at the site of relevance.

In this paper the turbulence box for the meandering process is generated using a transverse and vertical resolution of one diameter, whereas time resolution is 0.07sec. Further on, a second order time filter on the transverse wake position is applied in order to exclude contributions from turbulence scales smaller than two rotor diameters. The filter cut-off frequency and critical damping ratio is defined by

$$f_0 = \frac{U_0}{2D} \tag{1}$$

$$\xi = 0.7 \tag{2}$$

The defined lowpass frequency corresponds to a spatial filtering in which only turbulent scales exceeding two rotor diameters "survives" [7]. This has the physical explanation that atmospheric vortex structures smaller than 2D tend to change the deficit mixing process rather than contribute to distinct meandering.

2.1 How to handle multiple wakes in the DWM model

An important problem to address when modeling wake effects deep inside a wind farm is how to handle interacting wakes from multiple turbines. This is not straight forward, since the deficit from one turbine interferes with the next turbine and is further complicated by the turbulent mixing process that recovers energy downstream.

In order to investigate the interaction of wakes, excluding the effect of wake meandering, a simulation of a set of 5 turbines in a row with 8D spacing was studied for operating conditions of 8m/s and a turbulence intensity of 1%, see Figure 1. The inflow wind speed to each individual turbine was reduced with 2/3 at the rotor area - corresponding to the far field value for an ideal turbine with induction of 1/3

- and further expanded radially by 30% to account for wake pressure expansion. The quasi-steady wake deficit at the 8D downstream location behind each turbine was found using the axissymmetric flow solver described in [8], which is based on the eddy viscosity concept. This deficit was inserted successively in the same loop described above (wind speed reduction to 1/3, pressure expansion, flow solver) for the following downstream turbines, until the final deficit at the 40D downstream location was found.

The result is shown in Figure 2 together with deficits at 8D,16D,24D,32D and 40D downstream distances for a turbine operating at 8m/s. From the figure it can be seen that the final deficit has large similarities with the 8D deficit for small radial locations and significant similarities with the 40D deficit for large radial positions. This motivates a simple engineering approach for interacting wakes, where the strongest deficit at a given downstream location can be used when observing wakes from multiple turbines. This forms the basis for the selection approach formulated in equation (3). For a given downstream position in the wind farm $\mathbf{x}$, the resulting deficit is approximated by

$$u_{def,final}(\mathbf{x}) = \mathrm{MIN}(u_{def,i..N}(\mathbf{x})) \tag{3}$$

where i is turbine number from 1 to N turbines in the park.

The scales involved in the wake meandering process are very large and therefore assumed to be independent of flow disturbances from other turbines, since these mainly affects high frequencies, hence smaller vortex scales. The low frequent part of the turbulence corresponding to large vortex scales are to some extent similar for neighboring turbines, thus causing the wake pattern to meander in correlated traces. When turbines are positioned after each other in row, the downstream turbine only experience full wake conditions once in a while as illustrated in Figure 3, which further justifies the assumption of treating wake deficits individually as described in (3).

3 Relation between power production and ambient turbulence

A detailed description of the modeling of the quasi steady wake deficit in the DWM model can be found in [8], where also different validation cases against CFD Actuator Line (AL) model results are presented. Further work on validation of the DWM model was carried out within the European research project TOPFARM, where full scale measurements of power reduction in different wind farms as function of turbulence intensity became available. In Figure 4 the power reduction for the second turbine in a row relative to

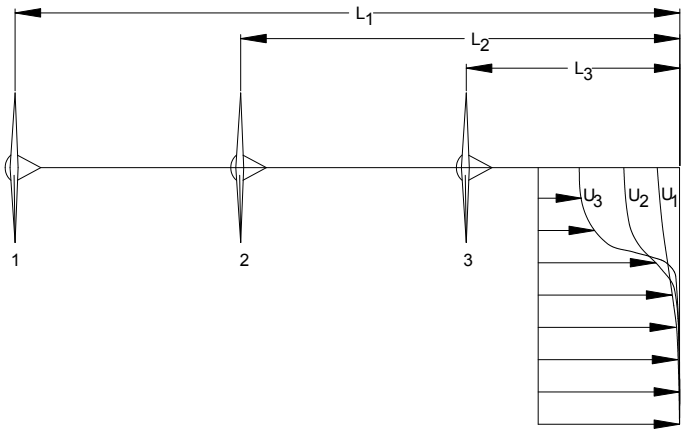

FIGURE 1: Illustration of individual deficits from multiple wind turbines in a row

the first turbine is shown as function of turbulence intensity for the wind direction aligned with the row. The data are extracted from three different wind farms with different turbine spacings. A strong influence of the turbulence intensity on the power deficit is seen. The parameters in the DWM model relating the ambient turbulent intensity to the eddy viscosity, were now recalibrated using this data set. The calibrated DWM model results are also shown in Figure 4, and results compare well with the measurements. In order to correlate the experimental analysis with model predictions it turned out to be very important to perform the load simulations covering the full range of measured wind speeds (6-12m/s) as well as the full direction sector ($\pm 5^\circ$) which were the conditions for the experimental data. The reason for this is the very non-linear performance of power performance with turbine load level and free- half- and full wake situation.

3.1 Measurements at the Egmond aan Zee wind farm

The Egmond Aan Zee wind farm is located outside the coast of the Netherlands, and it consists of 36 Vestas V90 3.0MW wind turbines installed on monopile foundations. The layout of the windfarm can be seen in Figure 5.

One meteorological mast is located at the site southwest of WT8, see Figure 5, which is the dominant wind direction at the site. The wind speed and direction is measured at three heights 116m, 70m and 21m, where 70m corresponds to the turbine hub height. In this work the wind direction sensors are calibrated based on power measurements of WT21, where lowest power production was expected at 196° due to the layout of the wind farm. The calibration of the met mast data is explained in details in [11], where an uncertainty level of 1.4° on the final measured wind direction is concluded. The SCADA data set includes electrical power, rotor rpm,

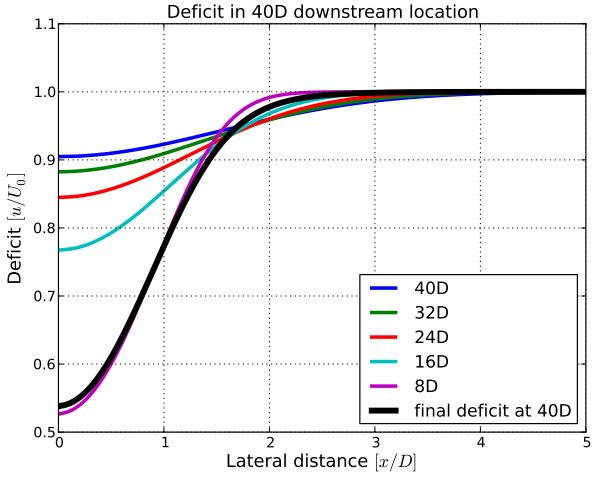

FIGURE 2: Multiple wakes are handled by observing the individual wakes from turbine 1 (U_1), 2 (U_2), 3 (U_3),.... The final deficit is a combination, where the part of the deficit leading to the highest wind speed reduction is applied as seen to the left. To the right is shown a comparison of deficits from 5 upstream turbines separated with 8 diameters calculated with the axissymmetric eddy viscosity model. The individual undisturbed deficits at the location of the 6^{th} turbine is shown together with a more correct approach handling effects of all upstream turbines. The ambient turbulence contribution to the wake expansion in this example is 2%, whereas meandering is not considered.

pitch angle, generator rpm, yaw orientation and nacelle wind speed.

Due to the location of the met-mast very close to the wind turbines, wake effects are preventing a correct recording of the free wind speed except for the free sector with wind directions ranging from south to west. In order to determine the free wind when the wind is from 319°, the nacelle cup anemometer on wind turbine 12 was used after first being calibrated against the met-mast for free wind directions, Figure 6. This clearly demonstrates that the nacelle wind speed at WT12 can be used to measure the free wind, which enables a measurement of wind speed for the 319° inflow case, where the met mast is affected by wakes.

In order to get a reliable measurement of the wind direction similar problems with met mast is faced. The wind vane of the met mast was therefore calibrated using a similar procedure as for the calibration of the WT12 nacelle wind speed. The power ratio between WT11 and WT12 is shown in Figure 7 as function of measured wind direction of the met mast. The wake direction is seen to be 319° using this sensor at 8m/s only, where small corrections are needed for different wind speeds. The conclusion is that the met mast can be used for the free wind direction, whereas the calibrated nacelle wind speed from WT12 and the calibrated wind direction from the met mast is used for the wake sector.

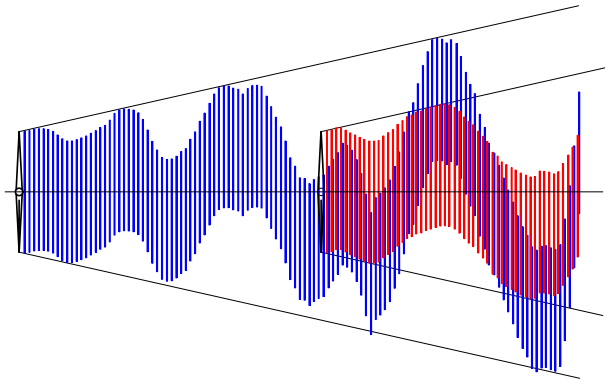

FIGURE 3: Illustration of wake pattern according to the DWM theory. The downstream turbine is only once in a while subjected to full wake loading.

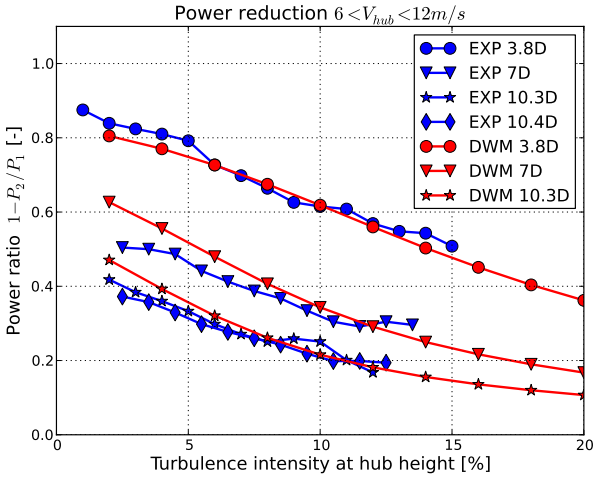

FIGURE 4: Power deficits as function of turbulence intensity measured for three different spacings and compared with DWM results. The experiments are carried out for three different wind farms; 3.8D=Wieringermeer (NL) [3], 7D+10.4D=Horns rev (DK) [4] and 10.3D=Nysted (DK) [5]

3.2 Comparison between HAWC2 simulations and measurements for a turbine in the wake sector

Full scale data extracted from the wake sector of 319° ± 5° have been compared with simulations. As previously de-

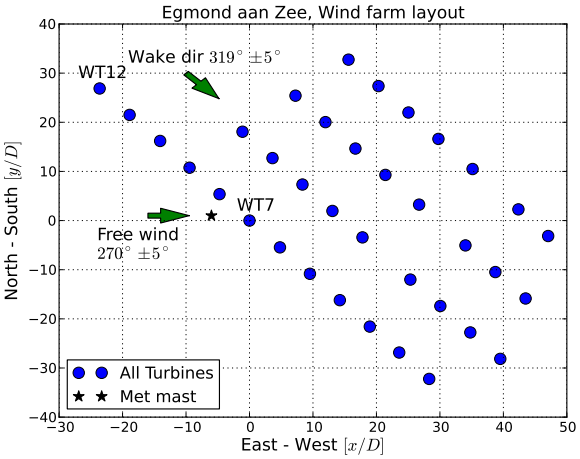

FIGURE 5: Position of turbines in farm relative to WT7. Distance is non-dim with rotor diameter.

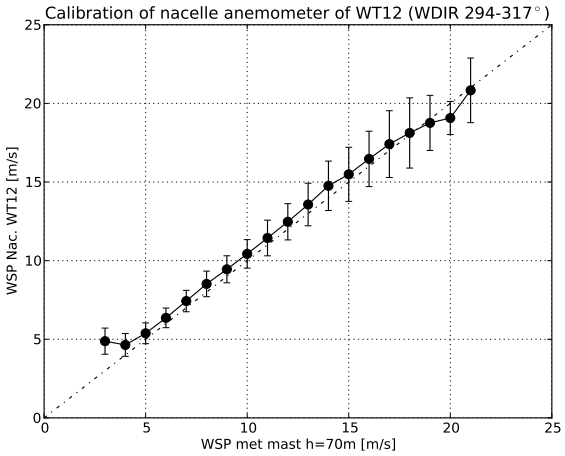

FIGURE 6: Left: Correlation between wind speed measured with nacelle mounted anemomenter on WT12 and met mast at hub height.

scribed, a problematic issue is that the met mast data cannot be used for this direction sector. This problem was solve as decribed in section 3.1 using the power production of WT12 as wind speed observer. Since the wind direction corresponding to the wake sector is more rare than corresponding to the free sector, each measurement point represent an average value of a sector of $\pm 5^\circ$ to obtain a suitable number of observations. In order to match the measurement conditions, simulations have been conducted using half-hour simulations with 3 different seed values (as for the free wind simulations), but further simulated at wind directions -5°,-2.5°,0°,2.5° and

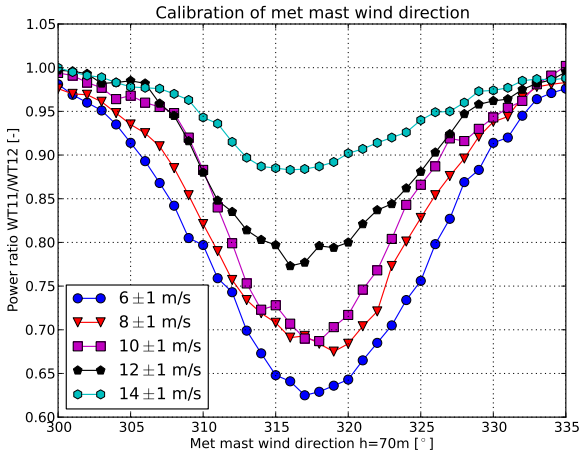

FIGURE 7: Power ratio between WT11 and WT12 for wind speed intervals; Whub=6, 8, 10, 12 and 14 ś1 m/s - as function of reference wind direction from the mast.

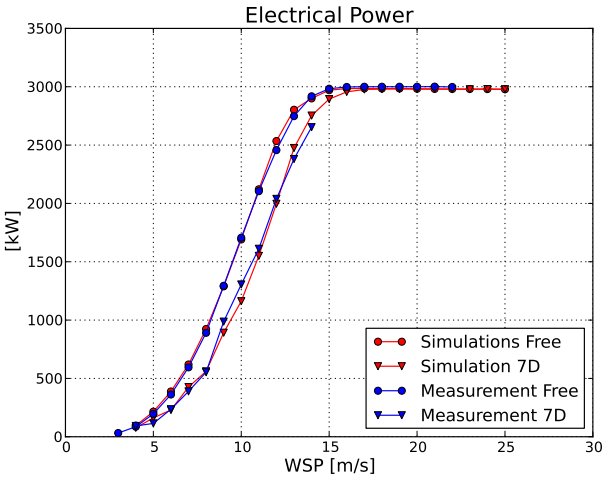

FIGURE 8: Power curve comparison between measurements and simulations is show for the free and 7D wake sector. A very fine agreement is seen

5° equal to -314°,-316.5°,319°,221.5° and 224°. The comparison of power curves is shown in Figure 8 for both free and wake sector. It is seen that the DWM model is capable of a very accurate prediction of the 7D wake condition for the WT7 turbine located as the fifth turbine in the row. This clearly demonstrates that the DWM approach is valid and fully mature with respect to detailed power preditions of wind turbines in wind farms.

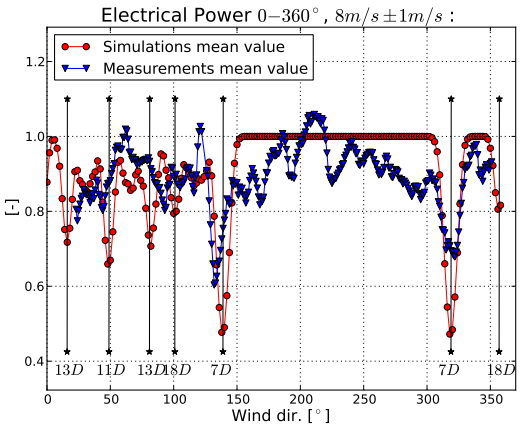

FIGURE 9: Power production of WT7 in DWM simulation as function of wind direction in the Egmond aan Zee Wind Farm. The wind speed is 8m/s at 6% ambient turbulence intensity. Results are non-dimensioned with the simulation result in the free sector

4 Power production as function of wind direction

For mean wind speeds between 7.5 and 8.5m/s, power production have been extracted from the measurement database as function of wind direction. Since there is only one met mast, the wind speed and the wind direction can unfortunately not be used for all directions. Therefore wind directions have been derived based on turbine orientation, and wind speeds were based on electrical power productions of turbines in free inflow conditions. The wind direction polar 0-360° is covered with a resolution of 2°, each consisting of three half hour simulations with different seeds for the turbulence generation. In general a fine agreement is observed showing a decrease in power production for the wake directions. However, the simulations seem to predict higher decrease in power for very narrow sectors around the wake direction than seen in measurements. One important factor is the statistical variation in wind direction ($\pm 2.5^\circ$) as well as ambient wind speed ($\pm 1 m/s$) not included in the simulations. The decrease in power productions is not only observed for row spacings of 7D, but power drops at 11 and 13D spacings are observed. Even at 18D small effects are seen, but these peaks seem to be of same magnitude in size of the general uncertainty level observed in the free sector.

5 Wind farm production as function of wind direction

Two sets of comparisons have been done for the full 0-360° direction polar. First simulated and measured total farm power has been compared. Simulations covering the 0-360° polar, with a resolution of 2° for each of the 36 turbines, including wake effects of all surrounding turbines has been compared to measurements in Figure 10. Each point in the measurements represents a wind interval of 5°. Therefore, the simulations are presented in two ways. First the raw results are shown, secondly a filtered dataset is shown. This filter consist of a simple window averaging of the direction observed and the neighboring points, thus corresponding to a wind sector of 5°. Clear power drops are seen in both measurements and simulations for the wind direction along the rows with 7D and 11D separation, respectively. In the simulations can also be seen effects attributed to 13D spacing, where this is more unclear in the measurements. In general a very good agreement is seen, which indicates the potential for using the DWM approach for wind farm production estimates too.

Differences in the power level can be seen for 7D spacings, where the simulation result in higher power reductions than seen in the measurements. Clearly this is a complicated load case, but a probable cause could be inaccuracies in determining a representative wind direction with a one-point observation for the full park, which has a spatial extend of up to 7km. Since the level of power drops in general are highly sensitive to the level of free- half- and full wake operation state, small errors in wind direction could have a large smoothening effect in this measurement presentation. Another error source might relate to the fact that we, for a given mean wind direction, assume a stationary stochastic turbulence process in the turbulence model used, whereas real life turbulence is instationary. The instationary part introduces direction trends and could also cause the wind direction far from the met mast to have a different mean value than assumed. A second aspect relates to the target spectra for the turbulence model, which is based on sub-inertial range only and originally fitted for 10min periods. If the energy content in the applied model is too low on the large scales, the meandering could be slightly underestimated causing a slightly conservative result. Finally, small differences in ambient turbulence intensity between measurements and simulation will cause differences in the power levels.

6 Influence of stability on the power production

Since the meandering, which is highly important for the wake load and power production, is mainly determined by the large turbulence scales in the ambient flow, it will also be sensitive to the ambient turbulence as well as to the atmospheric boundary layer stability conditions. In order to investigate this effect, the ambient turbulence field is modeled with an adaptation of the Mann spectral tensor to stability conditions other than neutral. For this purpose the Mann spectral tensor

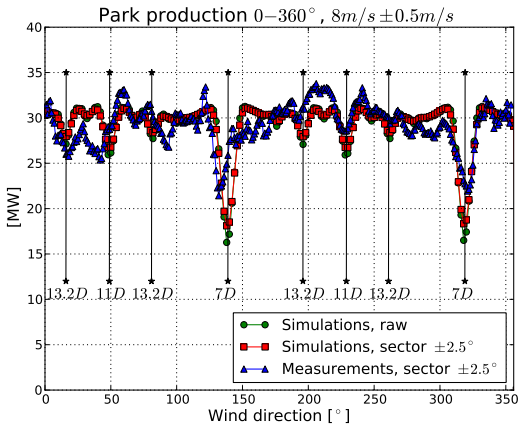

FIGURE 10: Total wind farm power production in the Egmond aan Zee Wind Farm at 8m/s $\pm$ 1m/s. Simulations are performed using an ambient turbulence level of 6%.

TABLE 1: Calibrated input parameters to the Mann turbulence model.

Stability class	L_M	Γ
Very unstable	108.3	3.3
Neutral	40.5	3.2
Very stable	9.3	4.4

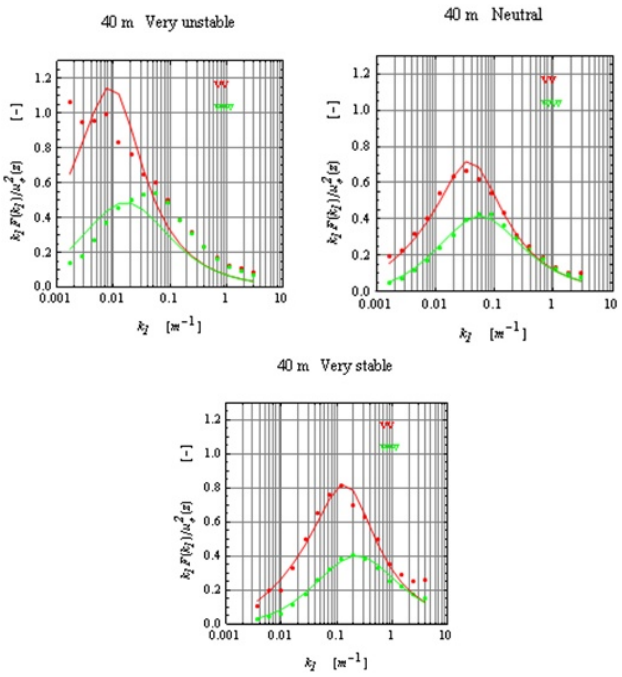

FIGURE 11: Comparison between target and simulated spectra for the cross wind component v and w. Unstable conditions are seen to increase the low frequent part of the spectra.

was fitted to turbulence spectre, measured for different stability classes at the Høvsøre site in Denmark, by adjusting the three parameters of the model: A length scale describing the size of the energy-containing eddies, L_M; a measure of the energy dissipation, $\alpha^{2/3}$, where α is the spectral Kolmogorov constant; and a parameter describing the degree of anisotropy, Γ. The fitting was done as described in [12], and the results are shown in Figure 11 and Table 1, respectively. In this study, the $\alpha^{2/3}$ determining the variance level is however bypassed by a turbulence scaling so the variance in the turbulence box matches exactly with the target turbulence intensity of the Egmond aan Zee conditions. An equal scaling in all directions are ensured to keep the structure of turbulence unaffected.

For each stability class, a total of 10 simulations were performed, each with a unique seed value for the stochastic turbulence simulation performed at 8m/s. This set of simulations was repeated for different wind directions covering both free, half and full wake situations. The influence on power output is shown in figure 13 and 14. In Figure 13 the turbulence intensity is 6% for all stability classes, and the impact on production is only due to the different level of energy in the low frequent part of the v and w turbulence spectra. In Figure 14, the ambient turbulence is changed according to the mean turbulence intensity related to the stability class. This means 3.5% for very stable, 5.5% for neutral and 6.5% for very unstable conditions as seen in Figure 12. Both figures show that stable condition causes a larger power drop in the full wake sector than for more unstable conditions. It is also seen that the variation in turbulence intensity has a higher impact on the production, than the length scale in itself. Especially Figure 14 show that the power drop for stable conditions are more narrow in terms of wind direction range than for the more unstable conditions. This effect can be explained by the magnitude of turbulence intensity in combination with the increased emphasis on the low frequent part of the spectrum controlling the wake meandering, hence the duration of time for the turbine operating in free, half and full wake conditions. Since the low frequent spectral energy content is largest for unstable conditions, the meandering related to unstable conditions also has the largest excursions, thus an increased production compared to stable conditions. Measurement of the power ratio are shown in Figure 15. Stable conditions are seen to give a slight reduction in power production, however the effect is smaller than seen in the simulations. The num-

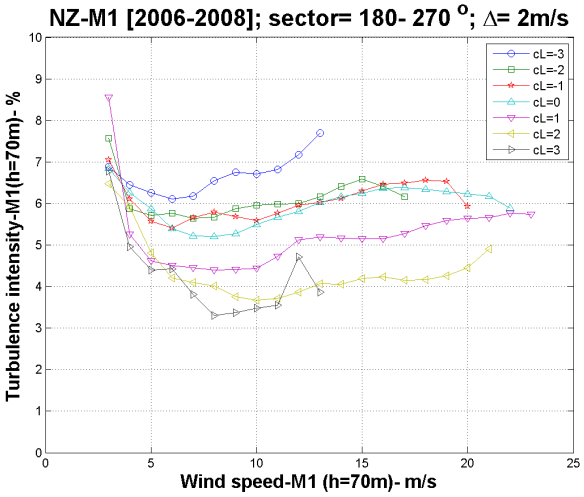

FIGURE 12: Measured mean turbulence intensity related to wind speed and stability class. CI=-3 for very unstable condition, CI=0 for neutral and CI=3.0 for very stable conditions.

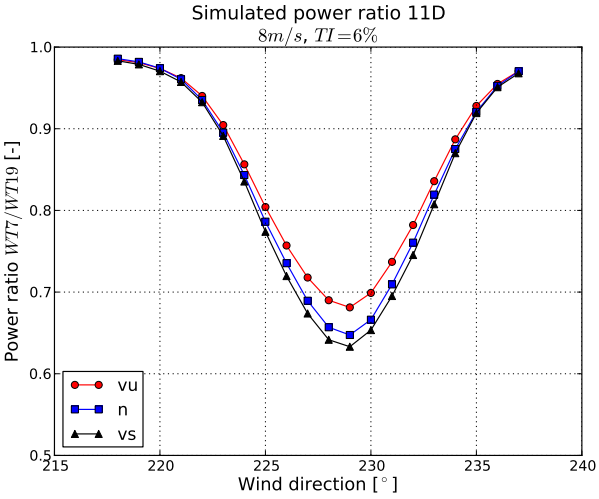

FIGURE 13: Power ratio of WT19/WT7 in 11D spacing simulated with different stability, however all simulated with a constant ambient turbulence intensity of 6%. Unstable conditions are seen to decrease the power drop compared to neutral or stable conditions.

ber of measured cases may, however, be too low to sort the measurement in these categories and should consequently only be used as indications for now. This is particularly true for the stable conditions related to mean wind directions in the range $[228° : 238°]$.

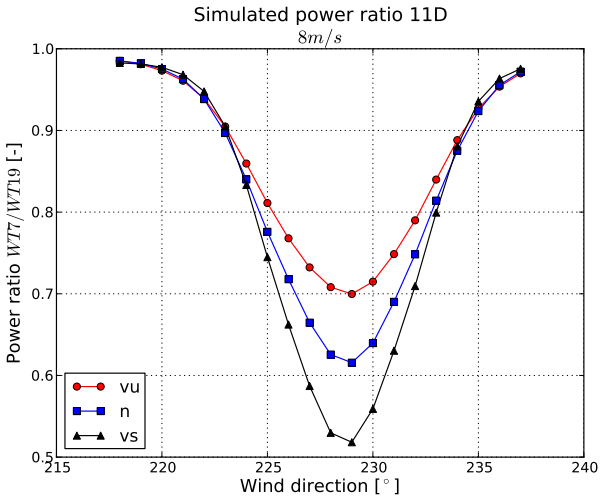

FIGURE 14: Power ratio of WT19/WT7 in 11D spacing as in Figure 13, however with a turbulence intensity matching the mean turbulence intensity for each stability class. This extra dimension related to the stability is seen to affect the power production level significantly.

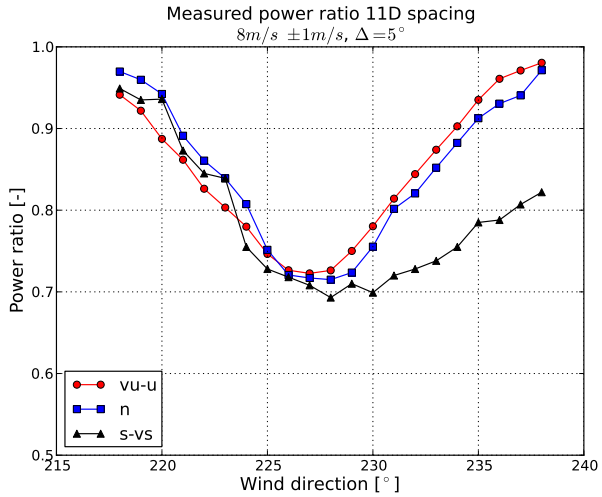

FIGURE 15: Measured power ratio of WT5/WT17, WT6/WT18, WT7/WT19 and WT8/WT20.

7 Conclusions

The DWM model implemented in the aeroelastic code HAWC2 has been extended for handling multiple wakes in an engineering approximation that also enables handling of wake meandering of multiple wakes. The model has subsequently been validated based on full scale turbine measurements of the Dutch wind farm Egmond aan Zee consisting of 36 Vestas V90 turbines. When comparing the predicted

power curves with measurements in both free and wake sector an excellent agreement is seen. This enables the conclusion that wake meandering caused by ambient turbulence is indeed an important contribution to the complex wake flow in wind farms, now verified with full scale measurements in situations with wakes from multiple upstream turbines. It is also seen that the model predict different power losses depending on the atmospheric stability. Unstable conditions are seen to lower the power loss, which is mainly caused by the increased meandering and turbulent mixing for these conditions.

REFERENCES

[1] Larsen, T. J. and Hansen, A., 2007, "How to HAWC2, the users manual," Tech. Rep. Risø-R-1597(en), Risoe National Laboratory - Technical University of Denmark.

[2] Larsen, T. J., Madsen, H., Larsen, G., and Hansen, K., 2012, "Evaluation of the Dynamic Wake Meander Model for Loads and Power Production in the Egmond aan Zee Wind Farm," Submitted to Wind Energy.

[3] Schepers, J., Obdam, T., and Prospathopoulos, J., 2011, "Analysis of wake measurements from the ECN Wind Turbine Test Site Wieringermeer, EWTW," Wind Energy, dOI: 10.1002/we.488.

[4] Hansen, K., Barthelmie, R.J., Jensen, L., and Sommer, A., 2011, "The impact of turbulence intensity and atmospheric stability on power deficits due to wind turbine wakes at Horns Rev wind farm," Wind Energy, dOI: 10.1002/we.512.

[5] Barthelmie, R. and Jensen, L., 2010, "Evaluation of wind farm efficiency and wind turbine wakes at the Nysted offshore wind farm," Wind Energy, **13**, pp. 573–586, doi: 10.1002/we.408.

[6] Rethore, P.-E., 2009, "Wind Turbine Wake in Atmospheric Turbulence." Tech. rep., Aalborg University, phD thesis.

[7] Larsen, G. C., Madsen, H. A., Thomsen, K., and Larsen, T. J., 2008, "Wake meandering - a pragmatic approach," Wind Energy, **11**, pp. 377–395.

[8] Madsen, H. A., Larsen, G., Larsen, T. J., and Troldborg, N., 2010, "Calibration and Validation of the Dynamic Wake Meandering Model for Implementation in an Aeroelastic Code." J. Sol. Energy Eng., **132(4)**, dOI: 10.1115/1.4002555.

[9] Larsen, G. C., Madsen, H. A., Bingöl, F., Mann, J., Ott, S., Sørensen, J., Okulov, V., Troldborg, N., Nielsen, M., Thomsen, K., Larsen, T., and Mikkelsen, R., 2007, "Dynamic wake modeling," Tech. Rep. Risø-R-1607(EN), Risoe National Laboratory - Technical University of Denmark.

[10] Taylor, G., 1937, "The spectrum of turbulence," Proc. R. Soc. Lond. A, **164**, pp. 476–490.

[11] Johansen, N., 2009, "Verification of simulated fatigue loads on wind turbines operating in wakes," Tech. Rep. MEK-FM-EP 2009-10, DTU MEK, master thesis.

[12] Mann, J., 1994, "The Spatial Structure of Neutral Atmospheric Surface-Layer Turbulence," Fluid Mech., **273**, pp. pp. 141–168.

ACKNOWLEDGMENT

The work has been funded by the European Commission in the framework of the Non-nuclear Energy Programme Sixth Framework and the contract No. REN07/FP6EN/S07.73680/038641 (TOPFARM - Next Generation Design Tool for Optimization of Wind Farm Topology and Operation). Vestas Wind Systems are acknowledged for the permissions to use the measurements, and the Danish EUDP project "Wake affected offshore tower and foundation loads" under contract 2010-1-10546, are acknowledged for funding the preparation of this paper.